Inorganic Chemistry

Article

pubs.acs.org/IC

Effect of N(4)-Phenyl Substitution in 2-Oxo-1,2-dihydroquinoline-3-carbaldehyde Semicarbazones on the Structure, DNA/Protein Interaction, and Antioxidative and Cytotoxic Activity of Cu(II) Complexes

Duraisamy Senthil Raja,[†] Nattamai S. P. Bhuvanesh,[‡] and Karuppannan Natarajan[†,*]

[†]Department of Chemistry, Bharathiar University, Coimbatore 641046 India

[‡]Department of Chemistry, Texas A&M University, College Station, Texas 77842, United States

Supporting Information

ABSTRACT: A new ligand, 2-oxo-1,2-dihydroquinoline-3-carbaldehyde semicarbazone (OQsc-H) (**1**);, its N(4)-phenyl derivative (OQsc-Ph) (**2**); and their corresponding copper(II) complexes $[CuCl_2(OQsc\text{-}H)]\cdot H_2O\cdot CH_3OH$ (**3**), $[CuCl_2(OQsc\text{-}Ph)(H_2O)]\cdot CH_3OH$ (**4**), and $[CuNO_3(OQsc\text{-}Ph)(H_2O)]NO_3\cdot H_2O\cdot C_2H_5OH$ (**5**) have been synthesized and characterized by structural, analytical, and spectral methods, in order to investigate the influence of N(4)-phenyl substitution on structure and pharmacological properties. In all of the complexes, the ligands coordinated to the Cu(II) ion in a neutral fashion via ONO donor atoms. The single-crystal X-ray structures of neutral complex (**3**) and cationic complex (**5**) exhibit a slightly distorted square-pyramidal structure, while neutral complex (**4**) revealed an octahedral structure. The interaction of the compounds with calf thymus DNA (CT-DNA) has been explored by absorption and emission titration methods, which revealed that compounds **1**−**5** could interact with CT-DNA through intercalation. A gel electrophoresis pictogram demonstrated the ability of the complexes (**3**−**5**) to cleave the pBR322 plasmid DNA through a hydrolytic process. The interactions of the compounds with bovine serum albumin (BSA) were also investigated using UV−visible, fluorescence, and synchronous fluorescence spectroscopic methods. The results indicated that all of the compounds could quench the intrinsic fluorescence of BSA in a static quenching process. Investigations of antioxidative properties showed that all of the compounds have strong radical scavenging potencies against hydroxyl radicals, 2,2-diphenyl-1-picrylhydrazyl radicals, nitric oxide, and superoxide anion radicals. Further, the cytotoxic effect of the compounds examined on cancerous cell lines such as human cervical cancer cells (HeLa), human laryngeal epithelial carcinoma cells (HEp-2), human liver carcinoma cells (Hep G2), human skin cancer cells (A431), and noncancerous NIH 3T3 mouse embryonic fibroblasts cell lines showed that all three complexes exhibited substantial cytotoxic activity. Further, all of the pharmacological investigations support the fact that there exists a strong influence of N(4)-phenyl substitution in semicarbazone.

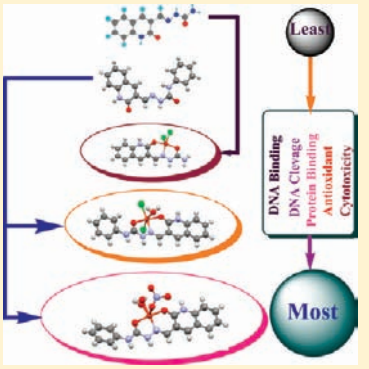

INTRODUCTION

Cancer is one of the main health concerns confronting humanity and one of the primary targets in therapeutic chemistry. So, the most rapidly developing area of pharmaceutical research is the discovery of drugs for cancer therapy. In this regard, cisplatin (*cis*-diamminedichloroplatinum(II)) is a promising and well-known metal-based drug for cancer therapy, but it has its own limitations because of the development of resistance in tumor cells and serious side effects such as nausea and kidney and liver failure typical of heavy metal toxicity.[1−5] So, more-efficient, less toxic, and target-specific noncovalent DNA binding anticancer drugs are to be developed. In general, anticancer agents that are approved for clinical use are molecules which damage DNA, block DNA synthesis indirectly through inhibition of nucleic acid precursor biosynthesis, or disrupt hormonal stimulation of cell growth.[6] Therefore, considerable attempts are being made to replace this drug with suitable alternatives, and hence numerous transition metal complexes have been synthesized and tested for their anticancer activities. Copper(II) complexes are regarded as the most promising alternatives to cisplatin as anticancer drugs; an idea supported by a considerable number of research articles describing the synthesis, DNA binding, and cytotoxic activities of numerous copper(II) complexes.[7−10] In addition, copper complexes which possess biologically accessible redox potentials and demonstrate high nucleobase affinity are potential reagents for the cleavage of DNA.[11−15] The ability of copper complexes to cleave DNA under physiological conditions has also received considerable attention because of the possible utility in highly targeted photodynamic therapeutic applications.[16−18] In the field of photodynamic therapy, Chakravarty and his co-workers have reported that the ternary Schiff base copper(II) phenathroline, which binds strongly to the minor

Received: September 17, 2011
Published: November 10, 2011

Scheme 1. Preparation Routes of the Ligands (1, 2) and Copper(II) Complexes (3, 4, and 5)

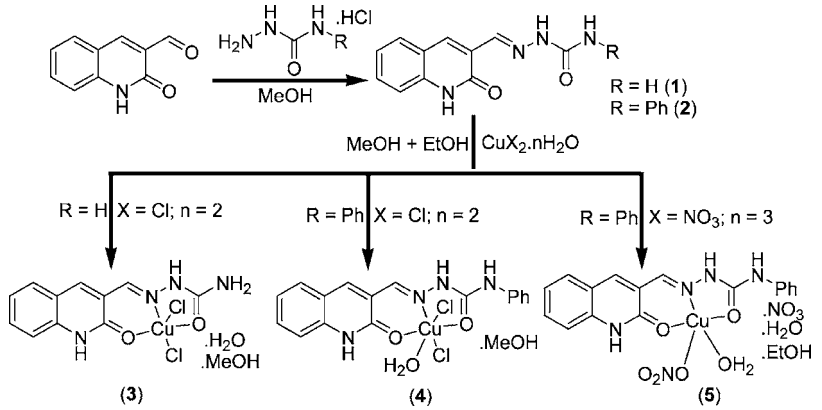

groove of bacterial DNA, exhibited both photonuclease (312 and 532 nm) and chemical nuclease activity under aerobic conditions without an additional oxidant.[18,19] Extending this approach, excitation into sulfur-to-Cu(II) charge transfer transitions, and, remarkably, weak Cu(II) ligand-field bands (600−750 nm), results in the formation of $^1O_2$ and generation of a relaxed circular DNA product.[18] Analogous compounds containing planar heterocyclic bases also show hydrolytic DNA cleavage activity under dark conditions,[20,21] indicating that the continued development of such constructs may lead to multifunctional metallonuclease models.

On the other hand, drug interactions at the protein binding level significantly affect the apparent distribution volume and their elimination rate. Therefore, the interactions of metal complexes with serum albumins have received much attention in the scientific community by studying antitumoral metallopharmaceutical pharmacokinetics and structure−activity relationships.[22] Bovine serum albumin (BSA) is the most extensively studied serum albumin, due to its structural homology with human serum albumin (HSA). This fact further supports the value of studying the interaction behavior of the metal complexes with bovine serum albumin (BSA) protein, while evaluating their anticancer properties.

On moving into the ligand point of view, it can be said that the semicarbazones as well as their derivatives are a class of ligands presenting a wide range of biological applications. Specifically, the semicarbazones have been screened for their antibacterial, antioxidant, antiproliferative, antimalarial, antitrypanosomal, anticonvulsant, and antitumoral activities.[23−28] Interestingly, the activity of these ligands might be enthused by coordination to some metal ions.[29] Particularly, copper(II) complexes containing semicarbazone ligands have displayed a wide spectrum of biological properties.[30−32]

Though there have been a large number of metal complexes reported along with their pharmacological properties, any attempt made to explain the factors that are responsible or affect their activity is relatively less existent. In this regard, we have recently found and reported that the N(4)-phenyl substitution not only altered the mode of coordination of 2-oxo-1,2-dihydroquinoline-3-carbaldehyde thiosemicarbazone but also enhanced the activities such as protein binding, radical scavenging, and cytotoxicity of its Cu(II) complex.[32] Moreover, only a little attention has been paid to the coordination chemistry of copper(II) with 2-oxo-quinoline-3-carbaldehyde Schiff base ligands recently. These Cu(II) complexes have been shown to have interesting pharmacological properties such as DNA binding, DNA cleavage, protein binding, antioxidation, and cytotoxicity.[33−36] And also, no attempts were made to explore the biological properties of 2-oxo-1,2-dihydroquinoline-3-carbaldehyde semicarbazones and their metal complexes. All of the above facts have stimulated our interest in the present work on synthesizing the new ligand, 2-oxo-1,2-dihydroquinoline-3-carbaldehyde semicarbazone, and its N(4)-phenyl derivative to better understand their coordination behavior toward Cu(II) ions and to evaluate the biological properties of the resulted Cu(II) complexes. The synthetic routes of the ligands and the Cu(II) complexes are shown in Scheme 1.

EXPERIMENTAL SECTION

Materials and Instrumentation. All starting precursors were of analytical grade, and double-distilled water was used throughout the experiments. 2-Oxo-1,2-dihydroquinoline-3-carbaldehyde was prepared according to the literature procedure.[37] The reagents and solvents were purchased commercially and used without further purification unless otherwise noted. Calf thymus DNA (CT-DNA), bovine serum albumin (BSA), and ethidium bromide (EB) were obtained from Sigma-Aldrich and used as received. Elemental analyses (C, H, N) were performed on Vario EL III Elemental Analyzer instrument. IR spectra (4000−400 cm^{-1}) were recorded on a Nicolet Avatar Model FT-IR spectrophotometer. ^1H NMR spectra of the ligands were recorded on a Bruker AMX 500 at 500 MHz. Melting points (Mp) of the compounds were determined with a Lab India instrument. Electronic absorption spectra were recorded using a Jasco V-630 spectrophotometer. Emission spectra were measured with a Jasco FP 6600 spectrofluorometer. The EPR spectra were recorded on a Bruker spectrometer operating at the X-band using 100 kHz magnetic field modulation. Solid state magnetic susceptibility measurements were carried out at room temperature on a Faraday balance calibrated using mercury(II) tetrathiocyanatocobaltate(II) as a calibrant under a magnetic field of 1.0 T. Diamagnetic corrections were estimated from Pascal tables.[38] Molar conductivity (Λ_M) measurements have been carried out on a Systronic conductivity bridge with a dip-type cell, using 1 mM solution of complexes in 5% aqueous DMSO.

Preparation of the Ligands. *2-Oxo-1,2-dihydroquinoline-3-carbaldehyde Semicarbazone (OQsc-H; 1).* Semicarbazide hydrochloride (1.12 g, 0.01 mol) dissolved in warm methanol (50 mL) was added to a methanol solution (50 mL) containing 1.73 g (0.01 mol) of 2-oxo-1,2-dihydroquinoline-3-carbaldehyde. The mixture was refluxed for 30 min, during which a pale yellow precipitate was formed. The reaction mixture was then cooled to room temperature, and the solid compound was filtered off. It was then washed with methanol and dried under vacuum conditions. Yield = 89%. Mp: 287 °C. Anal. Calcd for $C_{11}H_{10}N_4O_2$: C, 57.39; H, 4.38; N, 24.34%. Found: C, 57.41; H, 4.38; N, 24.31%. IR (KBr disks, cm^{-1}): 3173(ms) ν(NH); 1648(s) ν(C═O); 1576(s) ν(C═N). UV−visible (solvent, 5% DMSO and

dx.doi.org/10.1021/ic2020308 | Inorg. Chem. 2011, 50, 12852−12866

Table 1. Experimental Data for Crystallographic Analyses

compound	**2**·CH_3OH	**3**	**4**	**5**
empirical formula	$C_{18}H_{18}N_4O_3$	$C_{12}H_{16}Cl_2CuN_4O_4$	$C_{18}H_{20}Cl_2CuN_4O_4$	$C_{19}H_{24}CuN_6O_{11}$
fw	338.36	414.73	490.82	575.98
temp (K)	110(2)	110(2)	110(2)	110(2)
wavelength (Å)	1.5418	1.54178	0.71073	0.71073
cryst syst	monoclinic	monoclinic	orthorhombic	orthorhombic
space group	*P*2(1)/*c*	*C*2/*c*	*Pccn*	P2(1)2(1)2(1)
unit cell dimensions				
a (Å)	16.1489(9)	19.295(4)	29.236(15)	8.2583(13)
b (Å)	5.5421(3)	10.3068(16)	10.077(5)	11.2714(17)
c (Å)	22.5087(13)	17.634(4)	13.690(7)	25.413(4)
α (deg)	90	90	90	90
β (deg)	126.698(3)	118.340(19)	90	90
γ (deg)	90	90	90	90
volume ($Å^3$)	1615.22(16)	3086.4(10)	4033(4)	2365.5(6)
Z	4	8	8	4
density(calcd) (Mg/m^3)	1.391	1.785	1.617	1.617
abs. coeff. (mm^{-1})	0.801	5.430	1.381	0.996
F(000)	712	1688	2008	1188
cryst size (mm^3)	0.50 × 0.06 × 0.06	0.20 × 0.06 × 0.03	0.50 × 0.40 × 0.20	0.33 × 0.18 × 0.10
θ range for data collection (deg)	3.41 to 60.00	5.02 to 59.99	1.39 to 27.50	1.60 to 27.50
reflns collected	14419	5788	43011	27333
independent reflns	2326 [R(int) = 0.0545]	2144 [R(int) = 0.0547]	4605 [R(int) = 0.0683]	5402 [R(int) = 0.0362]
absorption correction	semiempirical from equivalents			
max. and min transmission	0.9535 and 0.6902	0.8541 and 0.4098	0.7697 and 0.5451	0.9105 and 0.7347
refinement method	full-matrix least-squares on F^2			
data/restraints/params	2326/0/227	2144/0/204	4605/0/263	5402/0/345
goodness-of-fit on F^2	0.965	0.954	1.052	1.039
final R indices [$I > 2\sigma(I)$]	R1 = 0.0367, wR2 = 0.0899	R1 = 0.0482, wR2 = 0.1269	R1 = 0.0338, wR2 = 0.0846	R1 = 0.0261, wR2 = 0.0685
R indices (all data)	R1 = 0.0471, wR2 = 0.0940	R1 = 0.0663, wR2 = 0.1359	R1 = 0.0405, wR2 = 0.0886	R1 = 0.0281, wR2 = 0.0696

95% Tris−HCl buffer, nm) (ε, M^{-1} cm^{-1}): 318 (18000); 355 (19464). ^{1}H NMR (DMSO−D_6, ppm): 11.92 (s, 1H, N(3)H); 11.43 (s, 1H, N(1)H); 8.59 (s, 1H, C(1)H); 8.07 (s, 1H, C(6)H); 7.63−7.65 (d, 1H, C(10)H); 7.46−7.51 (t, 1H, C(9)H); 7.29−7.31 (d, 1H, C(7)H); 7.17−7.22 (t, 1H, C(8)H); 6.56 (s, 2H, N(4)H_2).

2-Oxo-1,2-dihydroquinoline-3-carbaldehyde N-Phenylsemicarbazone (OQsc-Ph; 2). Compound **2** was prepared using the same procedure as described for **1** using 1.88 g (0.01 mol) of 4-phenylsemicarbazide hydrochloride and 1.73 g (0.01 mol) of 2-oxo-1,2-dihydroquinoline-3-carbaldehyde. The yellow compound obtained was separated. Yield = 91%. Mp: 306 °C. Anal. Calcd for $C_{17}H_{14}N_4O_2$: C, 66.66; H, 4.61; N, 18.29%. Found: C, 66.59; H, 4.65; N, 18.31%. IR (KBr disks, cm^{-1}): 3374(ms) ν(NH); 1657(s) ν(C═O); 1538(s) ν(C═N). IR (solvent, 5% DMSO and 95% Tris−HCl buffer, nm; ε, M^{-1} cm^{-1}): 362 (19356). ^{1}H NMR (DMSO−D_6, ppm): 11.99 (s, 1H, N(3)H); 10.93 (s, 1H, N(2)H); 8.93 (s, 1H, N(4)H); 8.75 (s, 1H, C(1)H); 8.20 (s, 1H, C(6)H); 7.01−7.73 (m, 9H, aromatic). Yellow colored single crystals suitable for X-ray diffraction studies were obtained from slow evaporation of a solution of **2** in a DMF/methanol mixture.

Synthesis of Cu(II) Complexes. Complexes [$CuCl_2$(OQsc-H)]·H_2O·CH_3OH (**3**), [$CuCl_2$(OQsc-Ph)(H_2O)]·CH_3OH (**4**), and [$CuNO_3$(OQsc-Ph)(H_2O)]NO_3·H_2O·C_2H_5OH (**5**) were synthesized by refluxing an equimolar amount of ethanolic solutions of appropriate metal salts $CuCl_2$·$2H_2O$ (85 mg, 0.5 mmol) or $Cu(NO_3)_2$·$3H_2O$ (121 mg, 0.5 mmol) with the methanolic solutions of respective ligands, OQsc-H (**1**) (115 mg, 0.5 mmol) or OQsc-Ph (**2**) (153 mg, 0.5 mmol), for 30 min (Scheme 1). Green colored crystals suitable for X-ray studies were obtained on slow evaporation of the reaction mixture for several days in all three cases. They were filtered off, washed with cold methanol, and dried under vacuum conditions.

Complex ***3***. Yield = 87%. Mp: 311 °C. Anal. Calcd for $C_{12}H_{16}Cl_2CuN_4O_4$: C, 34.75; H, 3.89; N, 13.51%. Found: C, 34.72; H, 3.86; N, 13.49%. IR (KBr disks, cm^{-1}): 3172(ms) ν(NH); 1638(s) ν(C═O); 1551(s) ν(C═N). UV−visible (solvent, 5% DMSO and 95% Tris−HCl buffer, nm; ε, M^{-1} cm^{-1}): 368 (23820). EPR (300K, 'g' value): 2.11 (solid), 2.09 (5% aq. DMSO). μ_{eff} (300K): 1.73 μ_B. Λ_M (S mol^{-1} cm^2): 1.21.

Complex ***4***. Yield = 90%. Mp: 312 °C. Anal. Calcd for $C_{18}H_{20}Cl_2CuN_4O_4$: C, 44.05; H, 4.11; N, 11.41%. Found: C, 44.12; H, 4.10; N, 11.46%. IR (KBr disks, cm^{-1}): 3377(ms) ν(NH); 1630(s) ν(C═O); 1499(s) ν(C═N). UV−visible (solvent, 5% DMSO and 95% Tris−HCl buffer, nm; ε, M^{-1} cm^{-1}): 372 (23700). EPR (300K, 'g' value): 2.15 (solid), 2.17 (5% aq. DMSO). μ_{eff} (300K): 1.69 μ_B. Λ_M (S mol^{-1} cm^2): 0.76.

Complex ***5***. Yield = 88%. Mp: 316 °C. Anal. Calcd for $C_{19}H_{24}CuN_6O_{11}$: C, 39.62; H, 4.20; N, 14.59%. Found: C, 39.71; H, 4.18; N, 14.58%. IR (KBr disks, cm^{-1}): 3373(ms) ν(NH); 1633(s) ν(C═O); 1510(s) ν(C═N). UV−visible (solvent, 5% DMSO and 95% Tris−HCl buffer, nm; ε, M^{-1} cm^{-1}): 395 (23152). EPR (300K, 'g' value): 2.19 (solid), 2.14 (5% aq. DMSO). μ_{eff} (300K): 1.71 μ_B. Λ_M (S mol^{-1} cm^2): 103.52.

Single Crystal X-Ray Diffraction Studies. Single-crystal X-ray diffraction data of compounds **2**·CH_3OH, **3**, **4**, and **5** were collected on BRUKER GADDS 1000 X-ray (three-circle) diffractometer. Integrated intensity information for each reflection was obtained by reduction of the data frames with the program APEX2.[39] In **3**, the thermal ellipsoid of C50 was elongated, suggesting disorder. Efforts to model this disorder did not decrease the reliability factors; hence C50 and O51 were restrained to have the same thermal ellipsoids. In **5**, thermal parameters of O4, O6, and O30 were found elongated, suggesting disorder. While the disorder in O6 was successfully modeled, two other oxygen atoms were not effective (trials of disorder on O4 and O30 not only increased the number of parameters and restraints but also did not improve on the reliability factors; also the thermal ellipsoids remained elongated in the disordered model). Hydrogen atoms attached to N and O were located from the Fourier difference maps and were set riding on the respective parent atom. All

dx.doi.org/10.1021/ic2020308 | *Inorg. Chem.* 2011, 50, 12852−12866

non-hydrogen atoms were refined with anisotropic thermal parameters. The structures were refined (weighted least-squares refinement on F^2) to convergence.[40] Relevant data concerning data collection and details of structure refinement are summarized in Table 1.

DNA Binding Studies. All of the experiments involving the binding of compounds with CT-DNA were carried out in double distilled water with tris(hydroxymethyl)-aminomethane (Tris, 5 mM) and sodium chloride (50 mM) and adjusted to pH 7.2 with hydrochloric acid. A solution of CT-DNA in the buffer gave a ratio of UV absorbance of about 1.9 at 260 and 280 nm, indicating that the DNA was sufficiently free of protein. The DNA concentration per nucleotide was determined by absorption spectroscopy using the molar extinction coefficient value of 6600 M^{-1} cm^{-1} at 260 nm. The compounds were dissolved in a mixed solvent of 5% DMSO and 95% Tris−HCl buffer for all of the experiments. Absorption titration experiments were performed with a fixed concentration of the compounds (25 μM) while gradually increasing the concentration of DNA (5−25 μM). While measuring the absorption spectra, an equal amount of DNA was added to both the test solution and the reference solution to eliminate the absorbance of DNA itself. The same experimental procedure was followed for emission studies also. The emission spectra were monitored by keeping the excitation of the test compounds at 380 nm. EB-DNA experiments were conducted by adding our compounds to the Tris-HCl buffer of EB-DNA. The change in the fluorescence intensity was recorded. The excitation and the emission wavelengths were 515 and 607 nm, respectively.

DNA Cleavage Experiment. The cleavage of DNA was monitored using agarose gel electrophoresis. Supercoiled pBR322 DNA (100 μM) in 5% DMSO and 95% Tris buffer (5 mM, pH 7.2) with 50 mM NaCl was incubated at 37 °C in the absence and presence of compounds. The DNA, compound, and sufficient buffer were premixed in a vial, and the reaction was allowed to proceed for 2 h at 37 °C before the addition of ethylene glycol and loading onto an agarose gel. Agarose gel electrophoresis of plasmid DNA was performed at 50 V in 1% slab gels containing 0.5 μg mL^{-1} ethidium bromide in Tris buffer. DNA was visualized by photographing the fluorescence of intercalated ethidium bromide under a UV illuminator. The cleavage efficiency was measured by determining the ability of the compounds to convert the supercoiled (SC) DNA to the nicked circular (NC) form and linear circular (LC) form. After electrophoresis, the proportion of DNA in each fraction was estimated quantitatively from the intensities of the bands using the ALPHA IMAGERTM 2200 Gel Documentation System. The fraction of the original supercoiled DNA converted to NC and LC at the end of the reaction was calculated.

Protein Binding Studies. The excitation wavelength of BSA at 280 nm and the emission at 345 nm were monitored for the protein binding studies. The excitation and emission slit widths and scan rates were maintained constant for all of the experiments. A stock solution of BSA was prepared in 50 mM phosphate buffer (pH = 7.2) and stored in the dark at 4 °C for further use. A concentrated stock solution of the compounds was prepared as mentioned for the DNA binding experiments, except that the phosphate buffer was used instead of a Tris-HCl buffer for all of the experiments. Titrations were manually done by using a micropipet for the addition of the compounds. For synchronous fluorescence spectra also, the same concentrations of BSA and the compounds were used, and the spectra were measured at two different $\Delta\lambda$ values (difference between the excitation and emission wavelengths of BSA), such as 15 and 60 nm.

Antioxidant Assays. The 2,2-diphenyl-1-picrylhydrazyl (DPPH) radical scavenging activity of the compounds was measured according to the method of Blois.[41] The DPPH radical is a stable free radical having a λ_{max} at 517 nm. A fixed concentration of the experimental compound was added to a solution of DPPH in methanol (125 μM, 2 mL), and the final volume was made up to 4 mL with double distilled water. The solution was incubated at 37 °C for 30 min in the dark. The decrease in absorbance of DPPH was measured at 517 nm.

The hydroxyl radical scavenging activity of the compounds has been investigated using the Nash method.[42] *In vitro* hydroxyl radicals were generated with the Fe^{3+}/ascorbic acid system. The detection of hydroxyl radicals was carried out by measuring the amount of formaldehyde formed from the oxidation reaction with DMSO. The formaldehyde produced was detected spectrophotometrically at 412 nm. A mixture of 1.0 mL of an iron−EDTA solution (0.13% ferrous ammonium sulfate and 0.26% EDTA), 0.5 mL of EDTA solution (0.018%), and 1.0 mL of DMSO (0.85% DMSO (v/v) in 0.1 M phosphate buffer, pH 7.4) was sequentially added in the test tubes containing test solutions. The reaction was initiated by adding 0.5 mL of ascorbic acid (0.22%) and incubated at 80−90 °C for 15 min in a water bath. After incubation, the reaction was terminated by the addition of 1.0 mL of ice-cold trichloroacetic acid (17.5% w/v). Subsequently, 3.0 mL of Nash reagent was added to each tube and left at room temperature for 15 min. The intensity of the color formed was measured spectrophotometrically at 412 nm against a reagent blank.

The assay of nitric oxide scavenging activity was based on the method[43] where sodium nitroprusside in aqueous solution at physiological pH spontaneously generates nitric oxide, which interacts with oxygen to produce nitrite ions that can be estimated using the Greiss reagent. Scavengers of nitric oxide compete with oxygen, leading to reduced production of nitrite ions. For the experiment, sodium nitroprusside (10 mM) in phosphate buffered saline was mixed with a fixed concentration of the compound and incubated at room temperature for 150 min. After the incubation period, 0.5 mL of the Griess reagent containing 1% sulfanilamide, 2% H_3PO_4, and 0.1% N-(1-naphthyl) ethylenediamine dihydrochloride was added. The absorbance of the chromophore formed was measured at 546 nm.

The superoxide anion radical scavenging assay was based on the capacity of the compounds to inhibit formazan formation by scavenging the superoxide radicals generated in a riboflavin−light−nitroblue tetrazolium system.[44] Each 3 mL reaction mixture contained 50 mM sodium phosphate buffer (pH 7.6), 20 μg of riboflavin, 12 mM EDTA, 0.1 mg of nitroblue tetrazolium, and 1 mL of test solution (20−100 μg/mL). The reaction was started by illuminating the reaction mixture with different concentrations of the compounds for 90 s. Immediately after illumination, the absorbance was measured at 590 nm. The entire reaction assembly was enclosed in a box lined with aluminum foil. Identical tubes with the reaction mixture kept in the dark served as blanks.

For the above four assays, all of the tests were run in triplicate, and various concentrations of the compounds were used to fix a concentration at which the compounds showed in and around 50% of activity. In addition, the percentage of activity was calculated using the formula, % of suppression ratio = $[(A_0 - A_C)/A_0] \times 100$. A_0 and A_C are the absorbance in the absence and presence of the tested compounds, respectively. The 50% activity (IC_{50}) can be calculated using the percentage of activity.

***In Vitro* Anticancer Activity Evaluation by MTT Assays.** Cytotoxicity studies of the compounds along with cisplatin were carried out on human cervical cancer cells (HeLa), human laryngeal epithelial carcinoma cells (HEp-2), human skin cancer cells (A431), human liver carcinoma cells (Hep G2), and NIH 3T3 normal cells (mouse embryonic fibroblasts), which were obtained from National Centre for Cell Science, Pune, India. Cell viability was carried out using the MTT assay method.[45] The HeLa, HEp-2, A431, and Hep G2 cells were grown in Eagles minimum essential medium containing 10% fetal bovine serum (FBS), while NIH 3T3 fibroblasts were grown in Dulbeccos modified Eagles medium (DMEM) containing 10% FBS. For the screening experiment, the cells were seeded into 96-well plates in 100 μL of the respective medium containing 10% FBS, at a plating density of 10 000 cells/well, and incubated at 37 °C, under conditions of 5% CO_2, 95% air, and 100% relative humidity for 24 h prior to the addition of compounds. The compounds were dissolved in DMSO and diluted in the respective medium containing 1% FBS. After 24 h, the medium was replaced with the respective medium with 1% FBS containing the compounds at various concentrations and incubated at 37 °C under conditions of 5% CO_2, 95% air, and 100% relative humidity for 48 h. Triplication was maintained, and the medium not containing the compounds served as the control. After 48 h, 10 μL of MTT (5 mg/mL) in phosphate buffered saline (PBS) was added to each well and incubated at 37 °C for 4 h. The medium with MTT was

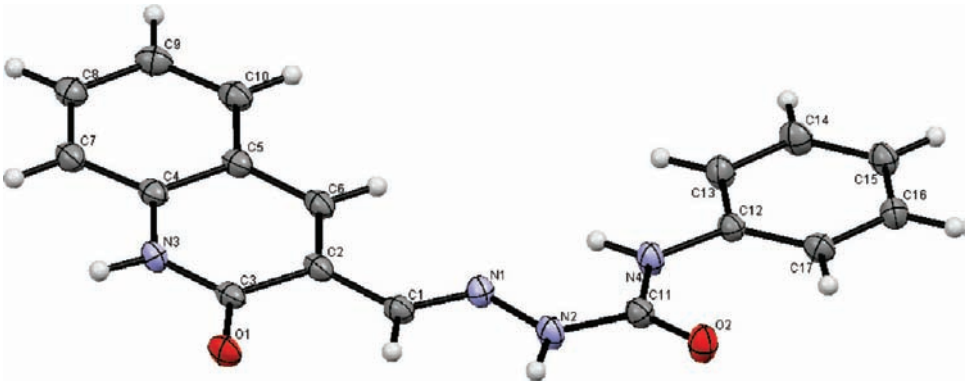

Figure 1. ORTEP diagram of **2**·CH_3OH. The thermal ellipsoids are drawn at 50% probability, and the methanol molecule has been omitted for clarity.

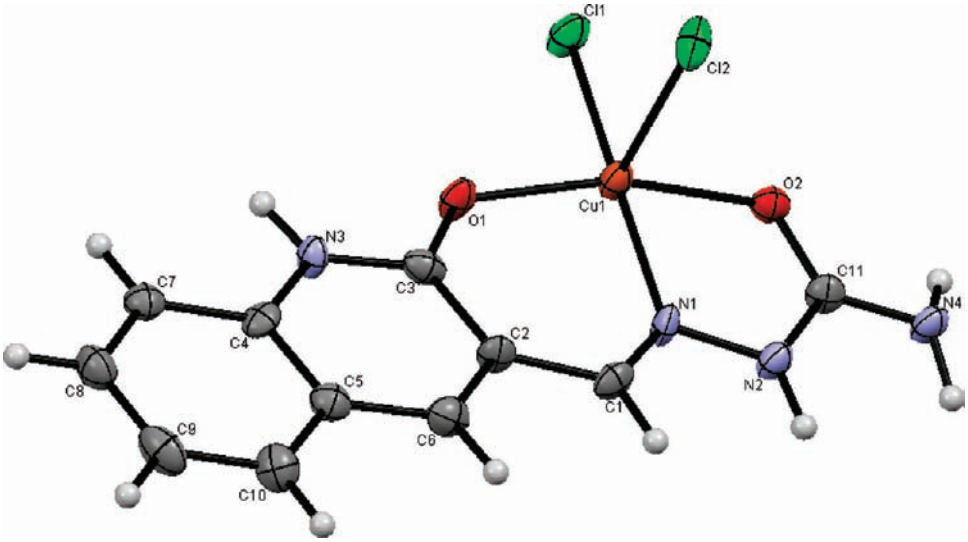

Figure 2. ORTEP diagram of **3**. The thermal ellipsoids are drawn at the 50% probability level. Methanol and water solvate molecules have been omitted for clarity.

then flicked off, and the formed formazan crystals were dissolved in 100 μL of DMSO. The absorbance was then measured at 570 nm using a microplate reader. The percentage of cell inhibition was determined using the following formula, and a graph was plotted with the percentage of cell inhibition versus concentration. From this, the IC_{50} value was calculated: % inhibition = [mean OD of untreated cells (control)/mean OD of treated cells (control)] × 100

RESULTS AND DISCUSSIONS

Synthesis and Chacterization. The ligands **1** and **2** were synthesized from the condensation reaction of 2-oxo-1,2-dihydroquinoline-3-carbaldehyde with hydrochloride salt of semicarbazide or 4-phenylsemicarbazide in a methanol medium as described in the Experimental Section. The structures of the ligands were confirmed by elemental analysis, IR and ^{1}H NMR (spectral techniques), and single crystal X-ray studies. Corresponding copper(II) complexes were obtained by the direct reaction of the ligand (**1** or **2**) with copper(II) salts, $CuCl_2·2H_2O$ or $Cu(NO_3)_2·3H_2O$, in a mixture of methanol and ethanol under reflux conditions, as mentioned in Scheme 1 (under the Experimental Section). Single crystals of the new copper(II) complexes were isolated by slow evaporation of the respective reaction mixture for several days. The complexes were obtained in a good yield and characterized by IR, elemental analysis, UV−visible, fluorescence spectroscopy, and EPR (see Experimental Section). All of the compounds are air-stable for extended periods and remarkably soluble in methanol, ethanol, DMF, and DMSO. Unlike, the other four compounds, complex **5** is highly soluble in water. The experimental μ_{eff} values of 1.73, 1.69, and 1.71 μ_B for complexes **3**, **4**, and **5**, respectively, revealed the presence of a +2 oxidation state of copper. In the X-band EPR spectra of the complexes at room temperature, a single isotropic resonance with "*g*" value of 2.11 and 2.09 for **3**, 2.15 and 2.17 for **4**, and 2.19 and 2.14 for **5** appeared for the powdered and for 5% aqueous DMSO solution of the complexes, respectively, indicating that the Cu(II) complexes retained their solid state structures in the aqueous solutions also. Moreover, the molar conductivities of copper(II) complexes in 5% aqueous DMSO have also been measured to find the labile nature of the coordinated chloride and nitrate in aqueous solution. The conductance values measured (Λ_M = 1.21 and 0.76 S mol^{-1} cm^2 for **3** and **4**, respectively) for **3** and **4** were too low to account for any dissociation. Hence, the two Cu(II) complexes **3** and **4** were considered nonelectrolytes and are quite stable in aqueous solution. However, a Λ_M of 103.52 S mol^{-1} cm^2 for **5** (103.52 S mol^{-1} cm^2) showed that the complex acts as a 1:1 electrolyte in aqueous solution. The

dx.doi.org/10.1021/ic2020308|*Inorg. Chem.* 2011, 50, 12852–12866

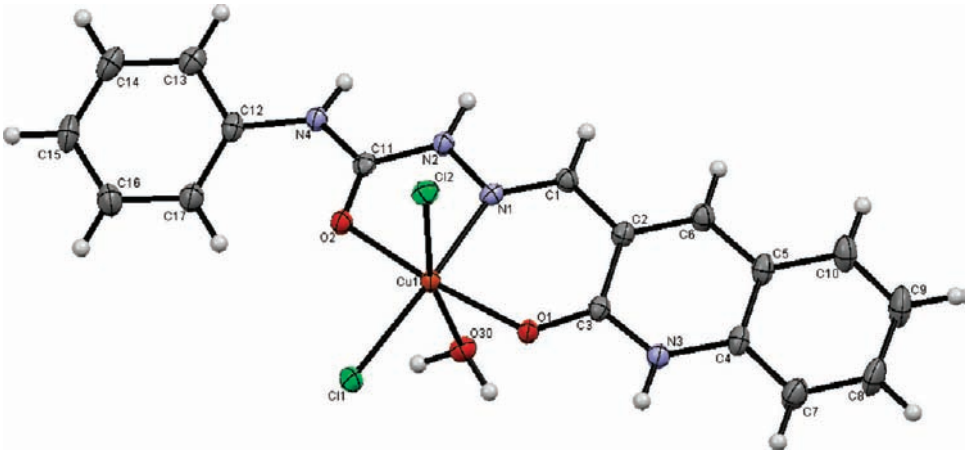

Figure 3. ORTEP diagram of **4**. The thermal ellipsoids are drawn at the 50% probability level, and the methanol molecule has been omitted for clarity.

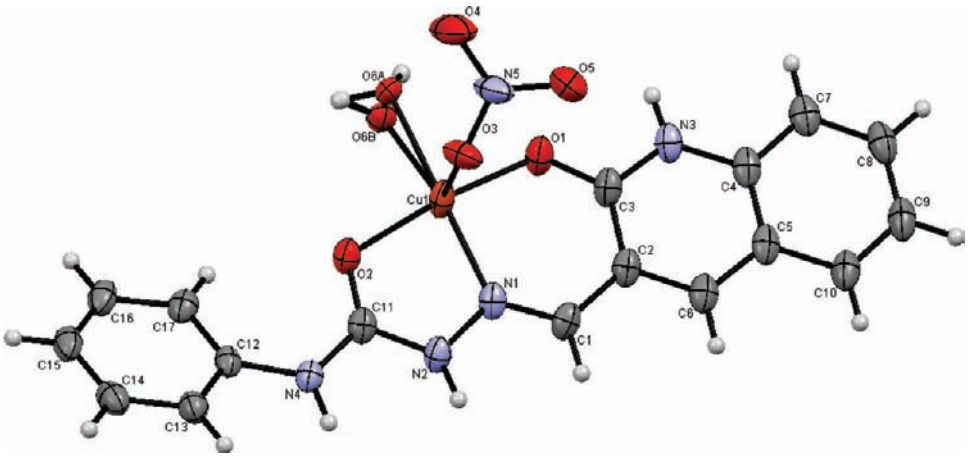

Figure 4. ORTEP diagram of **5**. The thermal ellipsoids are drawn at the 50% probability level. The nitrate ion, water, and ethanol molecules have been omitted for clarity.

structures of the new copper(II) complexes were finally confirmed by single crystal X-ray crystallographic studies.

Crystallography. An ORTEP representation of **2** is shown in Figure 1. The bond lengths and bond angles for **2**·CH_3OH are given in Table S1 (Supporting Information). The compound crystallizes in a monoclinic space group $P21/c$. The oxygen (O1) atom and the hydrazine nitrogen N1 are in a *trans* position with respect to the C11−N2 bond. The bond distances in the semicarbazone side chain agree well with the values observed for other semicarbazones where the C(11)═O(2) group is present in the keto form (1.2430(19) Å), and no large charge delocalization was detected, as shown by the clean double bond character of the C(1)−N(1) distance of 1.281(2) Å. In the crystal structure of **2**, though the molecule appears planar, the dihedral angle between the quinoline ring and phenyl ring is about of 8.52°, suggesting that the molecule has slight distortion in its planarity. A molecule of solvated methanol in the crystal lattice plays an important role in making the dimeric form of **2** through hydrogen bonding involving N2 and N3 nitrogen atoms and O1 and O2 oxygen atoms of the of **2**, along with the participation of oxygen (O31) of the methanol molecule. And there is no other hydrogen bonding between the dimeric units (Figure S1, Supporting Information).

The perspective ORTEP view of **3** with an atom numbering scheme is shown in Figure 2. Selected bond lengths and angles are summarized in Table S1 (Supporting Information). OQsc-H is coordinated to the copper ion in a neutral manner via ONO donor atoms, and the rest of the two coordination sites are occupied by chloride ions completing a square pyramidal geometry around the Cu(II) ion in **3**. A molecule of water and methanol as solvate molecules were also found in the asymmetric unit of the crystal lattice of **3**. Analysis of the shape determining angles α and β (the two largest angles around a Cu(II) ion) yields a value for the trigonality index, τ [$\tau = (\alpha - \beta)/60$], of 0.0842. According to it (τ = 0 and 1 for perfect square pyramidal and trigonal bipyramidal geometries, respectively), the geometry around Cu(II) can be described as a slightly distorted square pyramid. The copper(II) ion lies at about 0.187 Å above the average basal plane toward the axial Cl2 atom. The dihedral angle between the mean planes of the five-membered chelate ring and the six-membered one is 8.40°. In addition, there is an appreciable Jahn−Teller effect highlighted by an axial Cu−Cl2 distance (2.6473(18) Å) significantly longer than that observed for equatorial Cu−Cl1 distance (2.2273(16) Å). Since the semicarbazone moieties possess both the hydrogen bond donors as well as acceptors, the species provide the possibility of forming hydrogen bonds in the crystal. In fact, the crystal lattice of the complex showed a

dx.doi.org/10.1021/ic2020308 | *Inorg. Chem.* 2011, 50, 12852–12866

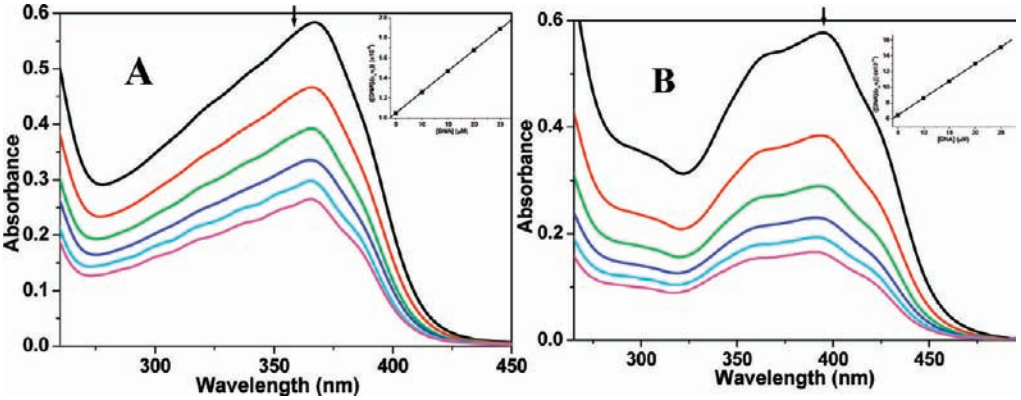

Figure 5. Changes in the electronic absorption spectra of **3** (A) and **5** (B) (25 μM) with increasing concentrations (0−25 μM) of CT-DNA. The inset shows a fitting of the absorbance data used to obtain the binding constants.

two-dimensional array in which each unit of the complex is hydrogen bonded to the other involving N2, N3, and N4 nitrogen atoms; O2, O20, and O51 oxygen atoms; and the Cl1 and Cl2 chlorine atoms (Figure S2, Supporting Information).

The molecular structure of complex $[CuCl_2(OQsc\text{-}Ph)(H_2O)]\cdot CH_3OH$ (**4**) together with the atom labeling scheme is depicted in Figure 3. The selected bond lengths and bond angles are listed in Table S1 (Supporting Information). The crystal structure of **4** consists of discrete neutral $[CuCl_2(OQsc\text{-}Ph)(H_2O)]$ complex molecules and methanol solvate molecules in which six donor atoms in an octahedral fashion (4 + 2) surround the copper(II) ion in the complex. The basal plane is made up from the O, N, and O atoms of the neutral tridentate semicarbazone ligand OQsc-Ph and one chloride ion, while the other chloride ion has taken one of the apical vertices; the remaining apical vertex has been occupied by the oxygen of the water molecule. The Cu(II) ion lies at about 0.086 Å slightly above the average basal plane toward the apical chloride ion. The dihedral angle between the mean planes of the five-membered chelate ring and the six-membered one is 5.47°, which ensures that the planarity of square should be appreciable. The axial Cu−Cl2 bond length (2.7088(14) Å) is significantly longer than that of the basal Cu−Cl1 bond length (2.2395(9) Å), which can be ascribed to Jahn−Teller distortion in **4**. The molecular packing suggests that the stabilization of the lattice must have been due to several hydrogen bonds, mainly involving the N2, N3, N4, O20, O30, Cl1, and Cl2 atoms (Figure S3, Supporting Information).

An ORTEP view of **5** together with the atom labeling scheme is depicted in Figure 4. The crystal building of **5** is made up of discrete monomeric entities containing a five-coordinated Cu(II) ion and nitrate ions. The quinoline oxygen and azomethine nitrogen together with the semicarbazide oxygen from the ligand OQsc-Ph coordinated as a neutral ONO chelating set form the basal plane. The fourth basal position is occupied by oxygen of the water molecule. The oxygen from a nitrate ion has taken the apical vertex. A slightly disordered square pyramidal geometry around the central copper cation has been observed, which is confirmed by the value for the trigonality index (τ) of 0.0568. A nitrate ion, one molecule of water, and ethanol have also been found in the asymmetric unit of the crystal lattice of **5**. The dihedral angle between the mean planes of the five-membered chelate ring and the six-membered one is 1.95°, which indicates that **5** has a more planar basal plane around the Cu(II) ion than those of complexes **3** and **4**. The crystal packing diagram of **5** presents a three-dimensional hydrogen-bond network, mainly involving the N2, N3, N4, O5, O6, O21, O22, O23, O30, and O31 atoms (Figure S4, Supporting Information).

It is to be noted that the free ligand OQsc-Ph shows that the O1 and N1 atoms are in a *trans* position with respect to the C11−N2 bond, but the rotation of 180° about the C11−N2 bond occurred in order to place the ONO functional groups on the same side, so as to coordinate as tridentate in the complex formation of **4** and **5**. In addition, the dihedral angle between the quinoline ring and the mean plane of the five- and six-membered chelate ring has been found to be 6.94, 6.26, and 0.63° for **3**, **4**, and **5**, respectively, which clearly suggested that the phenyl substitution at the N(4) position increases the planarity of the resulting Cu(II) complexes of **4** and **5**. The selected bond distances and bond angles of compounds **2**−**5** are given in Table S1 (Supporting Information) and agree well with those in related copper(II) complexes.[33−36]

CCDC 842872, CCDC 795275, CCDC 795276, and CCDC 842873 contain the supplementary crystallographic data for $\mathbf{2}\cdot CH_3OH$, **3**, **4**, and **5**, respectively. The data can be obtained free of charge via www.ccdc.cam.ac.uk/conts/retrieving.html (or from the Cambridge Crystallographic Data Centre, 12 Union Road, Cambridge CB2 1EZ, U.K.; fax (+44)1223−336−033 or e-mail deposit@ccdc.cam.uk).

DNA Binding Properties. It is a well-known fact that DNA is the primary pharmacological target of many antitumor compounds, and hence, the interaction between DNA and metal complexes is of paramount importance in understanding the mechanism. Thus, the mode and propensity for binding of compounds **1**−**5** to CT-DNA were studied with the aid of different techniques.

Absorption Spectral Studies. Electronic absorption spectroscopy is one of the most common ways to investigate the interaction of compounds with DNA. A compound binding to DNA through intercalation usually results in hypochromism with or without a small red or blue shift, due to the intercalative mode involving a strong stacking interaction between the planar aromatic chromophore and the base pairs of DNA.[33,34] The extent of hypochromism is commonly consistent with the strength of the intercalative binding interaction. The absorption spectral traces of compounds **1**−**5** (25 μM) with an increasing concentration of CT-DNA (0−25 μM) are shown in Figure S5A and B (Supporting Information), Figure 5A, Figure S5C (Supporting Information), and Figure 5B, respectively. Upon incremental additions of DNA to the test compounds, the following changes were observed. In the presence of DNA, the

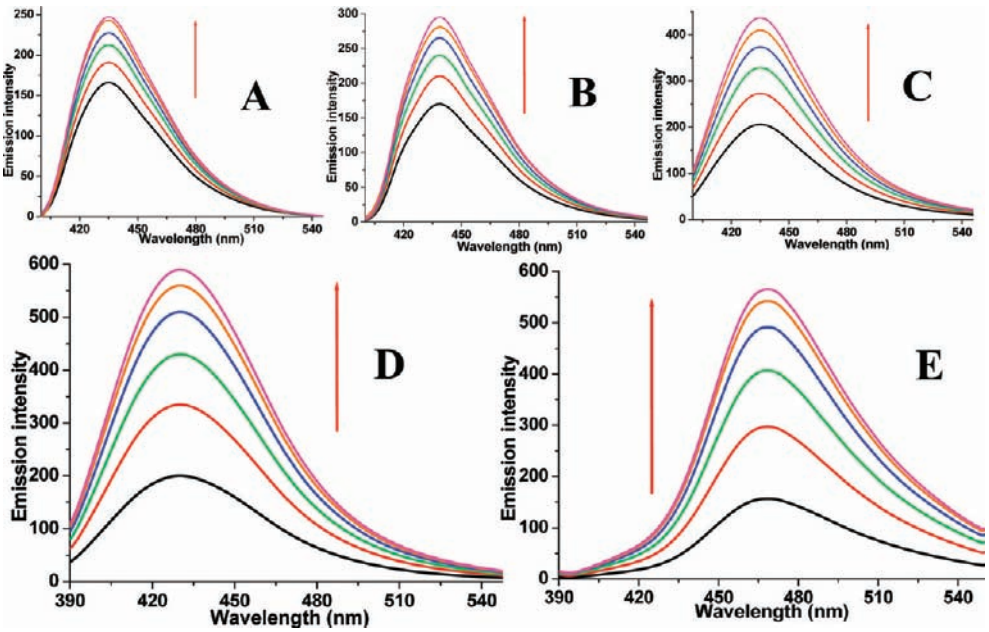

Figure 6. Emission enhancement spectra of compounds **1** (A), **2** (B), **3** (C), **4** (D), and **5** (E) (25 μM) in the presence of increasing amounts of CT-DNA (0, 5, 10, 15, 20, 25 μM; subsequent spectra). The arrow shows the emission intensity increases upon increasing the DNA concentration.

absorption bands of OQsc-H (**1**) exhibited a hypochromism of about 33.2% and 32.1% with a hypsochromic shift of 2 and 1 nm, respectively, at 318 and 355 nm, whereas the absorption band of **2** at 362 nm exhibited the same phenomenon of hypochromism of about 37.5% with a hypsochromic shift of about 2 nm. However, complexes **3** at 368 nm, **4** at 372 nm, and **5** at 395 nm exhibited a hypochromism of about 55.5%, 65.4%, and 71.4% with a hypsochromic shift of 3, 3, and 5 nm, respectively. These results suggested an intimate association of the test compounds with CT-DNA, and it is also likely that these compounds bind to the DNA helix via intercalation.[33,36] After the compounds intercalate to the base pairs of DNA, the π^* orbital of the intercalated compounds could couple with π orbitals of the base pairs, thus decreasing the $\pi \rightarrow \pi^*$ transition energies, hence resulting in hypochromism.[36] The complexes (**3**−**5**) showed more hypochromicity than the ligands (**1** and **2**), indicating that the binding strength of the copper(II) complexes is much stronger than that of the free ligands. In order to compare quantitatively the binding strength of the compounds, the intrinsic binding constants (K_b) of them with CT-DNA were determined from the following equation:

$$[\mathrm{DNA}]/(\varepsilon_a - \varepsilon_f) = [\mathrm{DNA}]/(\varepsilon_b - \varepsilon_f) + 1/K_b(\varepsilon_b - \varepsilon_f)$$

where [DNA] is the concentration of DNA in base pairs and the apparent absorption coefficient ε_a, ε_f, and ε_b correspond to A_{obs}/[compound], the extinction coefficient of the free compound, and the extinction coefficient of the compound when fully bound to DNA, respectively. The plot of [DNA]/($\varepsilon_a - \varepsilon_f$) versus [DNA] gave a slope and intercept which are equal to $1/(\varepsilon_b - \varepsilon_f)$ and $1/K_b(\varepsilon_b - \varepsilon_f)$, respectively; K_b is the ratio of the slope to the intercept. The magnitudes of intrinsic binding constants (K_b) were calculated to be 2.28(±0.11) × 10^4 M^{-1}, 4.92(±0.09) × 10^4 M^{-1}, 2.98(±0.13) × 10^5 M^{-1}, 4.08(±0.10) × 10^5 M^{-1}, and 6.72(±0.17) × 10^5 M^{-1} for compounds **1**, **2**, **3**, **4**, and **5**, respectively. The observed values of K_b revealed that the ligands and the Cu(II) complexes bind to DNA via the intercalative mode.[8,33,35] From the results obtained, it has been found that complex **5** strongly bound with CT-DNA relative to that with **4** and **3**, and the order of binding affinity is **3** < **4** < **5**. From the electronic absorption studies, though it has been found that the compounds can bind to DNA by intercalation, the binding mode needs to be proved through some more experiments.

Fluorescence Spectral Studies. To further confirm the interaction between the test compounds and CT-DNA, emission experiments were carried out. The results of fluorescence titration spectra have also been confirmed to be effective for characterizing the binding mode of the metal complexes to DNA.[33] Compounds **1**−**5** exhibited weak luminescence in the Tris−HCl buffer with a maximum wavelength of about 435, 439, 437, 430, and 468 nm, respectively, when excited at 380 nm. The results of the emission titration for the ligands and its corresponding Cu(II) complexes with CT-DNA that are illustrated in the titration curves are shown in Figure 6.

An increase in DNA concentration increases the emission intensity of the compounds. Upon incremental additions of CT-DNA, the emission intensity of ligands **1** and **2** at 435 and 439 nm increased by around 1.49 and 1.74 times, respectively, in comparison to the same in the absence of DNA, whereas with their corresponding complexes **3**, **4**, and **5** at 437, 430, and 468 nm, the intensities were increased by around 2.12, 2.95, and 3.62 times, respectively. This phenomenon is related to the extent to which the compound penetrates into the hydrophobic environment inside the DNA, thereby avoiding the quenching effect of solvent water molecules. The binding of free ligands and complexes to CT-DNA leads to a marked increase in the emission intensity, which also agrees with those observed for other intercalators.[33,34,36] These results showed that the complexes bound more strongly than the free ligands. The higher binding affinity of the Cu(II) complexes is attributed to the extension of the π system of the intercalated ligand due to the coordination with the Cu(II) ion. Since the complexes have greater planar area than that of the free ligand, the complexes

dx.doi.org/10.1021/ic2020308 | Inorg. Chem. 2011, 50, 12852–12866

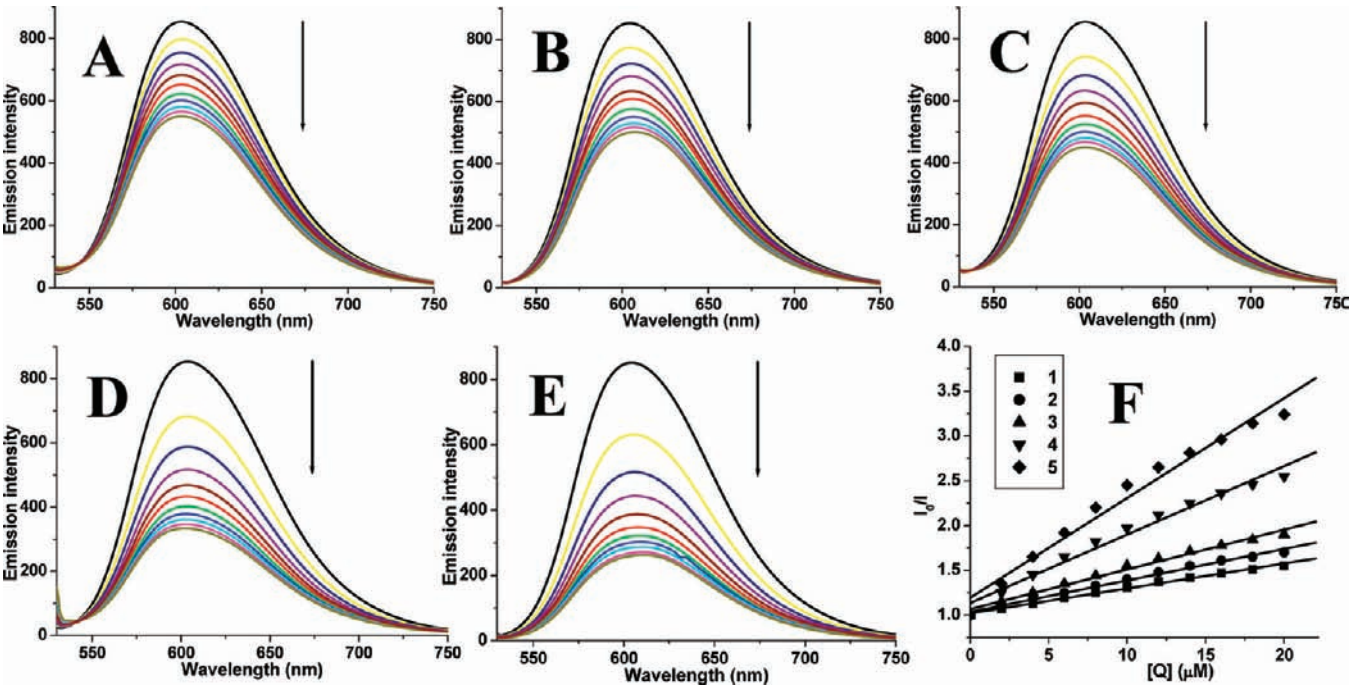

Figure 7. Fluorescence quenching curves of ethidium bromide bound to DNA: **1** (A), **2** (B), **3** (C), **4** (D), and **5** (E). [DNA] = 5 μM, [EB] = 5 μM, and [compound] = 0–20 μM. (F) Stern–Volmer plots of the fluorescence titrations of **1**, **2**, **3**, **4**, and **5**.

penetrate more deeply into and stack more strongly with the base pairs of the DNA.

Competitive Binding between Ethidium Bromide and Compounds 1–5 for CT-DNA. Steady-state competitive binding experiments using compounds **1**, **2**, **3**, **4**, and **5** as quenchers were undertaken to get final proof for the binding of the compounds to DNA via intercalation. Ethidium bromide (EB) is a planar cationic dye which is widely used as a sensitive fluorescence probe for native DNA. EB emits intense fluorescent light in the presence of DNA due to its strong intercalation between the adjacent DNA base pairs. The displacement technique is based on the decrease of fluorescence resulting from the displacement of EB from a DNA sequence by a quencher, and the quenching is due to the reduction of the number of binding sites on the DNA that are available to the EB. The fluorescence quenching spectra of DNA-bound EB by compounds **1**, **2**, **3**, **4**, and **5** shown in Figure 7 illustrate that, as the concentration of the compounds increases, the emission band at 602 nm exhibited hypochromism up to 35.5, 41.2, 47.4, 60.8, and 69.1% of the initial fluorescence intensity for **1**, **2**, **3**, **4**, and **5**, respectively. The observed decrease in the fluorescence intensity clearly indicates that the EB molecules are displaced from their DNA binding sites and are replaced by the compounds under investigation.[46] Quenching data were analyzed according to the following Stern–Volmer equation:

$$I_0/I = K_q[Q] + 1$$

where I_0 is the emission intensity in the absence of a quencher, I is the emission intensity in the presence of a quencher, K_q is the quenching constant, and [Q] is the quencher concentration.

The K_q value is obtained as a slope from the plot of I_0/I versus [Q]. The quenching plots illustrate that the quenching of EB bound to CT-DNA by free ligands and the copper(II) complexes are in good agreement with the linear Stern–Volmer equation. In the Stern–Volmer plots of I_0/I versus [Q] (Figure 7F), the K_q values for **1**, **2**, **3**, **4**, and **5** were found to be 1.78(±0.19) × 10^4 M^{-1}, 2.52(±0.15) × 10^4 M^{-1}, 8.32(±0.21) × 10^4 M^{-1}, 3.94(±0.24) × 10^5 M^{-1}, and 8.96(±0.33) × 10^5 M^{-1}, respectively. Further, the apparent binding constant (K_{app}) values obtained for the compounds using the following equation

$$K_{EB}[EB] = K_{app}[compound]$$

(where the compound concentration has the value at a 50% reduction of the fluorescence intensity of EB, K_{EB} = 1.0 × 10^7 M^{-1} and [EB] = 5 μM) were found to be 2.17(±0.14) × 10^4 M^{-1}, 4.53(±0.29) × 10^4, 2.91(±0.23) × 10^5 M^{-1}, 4.12(±0.16) × 10^5 M^{-1}, and 6.67(±0.21) × 10^5 M^{-1} respectively for **1**, **2**, **3**, **4**, and **5**, respectively. These data suggested that the interaction of the copper(II) complexes with CT-DNA is stronger than that of the free ligand, which is consistent with the above absorption and emission spectral observations. Since these changes indicate only one kind of quenching process, it may be concluded that all of the compounds bind to CT-DNA via the same mode. Furthermore, such quenching constants and binding constants of the ligands and Cu(II) complexes suggest that the interaction of all of the compounds with DNA should be intercalation.[33,34,36]

On the basis of all of the spectroscopic studies, we concluded that the free ligands and copper(II) complexes can bind to CT-DNA in an intercalative mode and that the Cu(II) complexes bind to CT-DNA more strongly than the free ligands. Among the two ligands, the one which has relatively more planar area and aromatic conjugation due to the presence of a phenyl ring in the N(4) position of OQsc-Ph showed greater binding affinity to DNA over the other ligand, OQsc-H. The same phenomenon has also been used to obtain the reason for the higher binding activity of complexes **4** and **5** over **3**, because the ligand coordinated as a neutral tridentate to Cu(II) in all three complexes, whereas the cationic complex nature of **5** is likely to

dx.doi.org/10.1021/ic2020308 | Inorg. Chem. 2011, 50, 12852–12866

be the reason for the observed highest affinity of **5** with DNA over **4**.

DNA Cleavage Studies. To assess the DNA cleavage ability of complexes **3**−**5**, supercoiled (SC) pBR322 DNA was incubated with two different concentrations of the compounds in a 5 mM Tris-HCl/50 mM NaCl buffer at pH 7.2 for 2 h without the addition of a reductant (Figure 8). Control

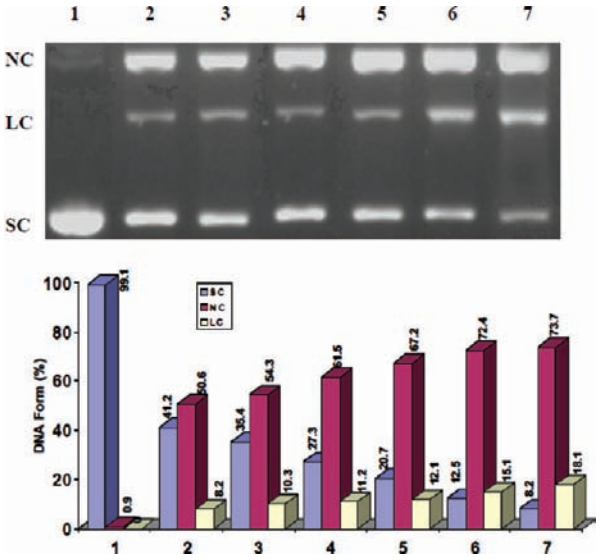

Figure 8. Gel electrophoresis diagram showing the hydrolytic cleavage of supercoiled pBR322 DNA by complexes **3**−**5** in 5% DMSO and 95% 5 mM Tris−HCl/50 mM NaCl buffer at pH 7.2 and 37 °C with an incubation time of 2 h. Lane 1: control. Lanes 2 and 3: **3** (10 and 20 μM). Lanes 4 and 5: **4** (10 and 20 μM). Lanes 6 and 7: **5** (10 and 20 μM). Relative amounts of the different DNA forms present in each lane are given in the lower part of the figure. Forms SC, NC, and LC are supercoiled, nicked circular, and linear circular DNA, respectively.

experiments showed that the ligands (OQsc-H and OQsc-Ph) and copper salts ($CuCl_2 \cdot 2H_2O$ and $Cu(NO_3)_2 \cdot 3H_2O$) were cleavage inactive. Upon gel electrophoresis, a concentration-dependent DNA cleavage was observed for all of the complexes; the SC DNA was converted into nicked circular (NC) DNA and linear circular (LC) DNA. Complex **5** showed greater DNA cleavage ability than the other two (**3** and **4**). In the case of **5**, when the concentration was increased from 10 μM to 20 μM, the production of the NC form of DNA was also increased from 72.4% to 73.7%, whereas the production of the LC form of DNA was increased from 15.1% to 18.1% (Figure 8). Similar types of cleavage behavior have also been observed for complexes **3** and **4**. The involvement of reactive oxygen species (hydroxyl, superoxide, singlet oxygen, and hydrogen peroxide) in the nuclease mechanism can be inferred by monitoring the quenching of the DNA cleavage in the presence of radical scavengers in solution. Complexes **3**−**5** did not show inhibition of DNA cleavage in the presence of scavengers of hydroxyl radicals (DMSO and mannitol), singlet oxygen (sodium azide and L-histidine), and superoxide radical scavengers (SOD). This indicates that the cleavage of DNA probably follows a hydrolytic cleavage mechanism. In addition, inhibition or promotion of DNA cleavage is not observed appreciably under aerobic and anaerobic conditions. This suggested that oxidative cleavage is not a factor. Hence, the DNA cleavage observed here is expected to occur through a hydrolytic process.[47]

Protein Binding Studies. *Fluorescence Quenching of BSA by Compounds 1*−*5.* Qualitative analysis of the binding of chemical compounds to BSA is usually detected by inspecting the fluorescence spectra. Generally, the fluorescence of BSA is caused by two intrinsic characteristics of the protein, namely tryptophan and tyrosine. Changes in the emission spectra of tryptophan are common in response to protein conformational transitions, subunit associations, substrate binding, or denaturation. Therefore, the intrinsic fluorescence of BSA can provide considerable information on their structure and dynamics and is often utilized in the study of protein folding and association reactions. The interaction of BSA with our compounds (**1**−**5**) was studied by fluorescence measurement at room temperature. A solution of BSA (1 μM) was titrated with various concentrations of the compound (0−50 μM). Fluorescence spectra were recorded in the range of 290−450 nm upon excitation at 280 nm. The effects of the compound on the fluorescence emission spectrum of BSA are shown in Figure 9.

The addition of the above compounds to the solution of BSA resulted in a significant decrease of the fluorescence intensity of BSA at 345 nm, up to 45.7, 51.9, 65.5, 71.7, and 78.7% from the initial fluorescence intensity of BSA accompanied by a hypsochromic shift of 4, 5, 5, 4, and 5 nm for **1**, **2**, **3**, **4**, and **5**, respectively. The observed blue shift is mainly due to the fact that the active site in protein is buried in a hydrophobic environment. This result suggested a definite interaction of all of the compounds with the BSA protein.[35,36]

Quenching can occur by different mechanisms, which are usually classified as dynamic quenching and static quenching; dynamic quenching refers to a process in which the fluorophore and the quencher come into contact during the transient existence of the excited state. Static quenching refers to fluorophore−quencher complex formation in the ground state. A simple method to explore the type of quenching is UV−visible absorption spectroscopy. UV−visible spectra of BSA in the absence and presence of the compounds (Figure 10) show that the absorption intensity of BSA was enhanced as the compounds were added, and there was a little blue shift of about 1, 1, 2, 2, and 3 for the compounds **1**, **2**, **3**, **4**, and **5**, respectively. It revealed that there exists a static interaction between BSA and the added compounds due to the formation of the ground state complex of the type of BSA-compound reported earlier.[48]

To study the quenching process further, fluorescence quenching data were analyzed with the Stern−Volmer equation and Scatchard equation. The quenching constant (K_q) can be calculated using the plot of I_0/I versus [Q] (Figure 11A). If it is assumed that the binding of compounds with BSA occurs at equilibrium, the equilibrium binding constant can be analyzed according to the Scatchard equation:

$$\log[(I_0 - I)/I] = \log K_{bin} + n\log[Q]$$

where K_{bin} is the binding constant of the compound with DNA and n is the number of binding sites.

From the plot of $\log(I_0 - I)/I$ versus log [Q] (Figure 11B), the number of binding sites (n) and the binding constant (K_{bin}) have been obtained. The calculated K_q, K_{bin}, and n values are given in Table 2. The calculated value of n is around 1 for all of the compounds, indicating the existence of just a single binding site in BSA for all of the compounds. The values of K_q and K_{bin} for all of the compounds suggested that the complexes interact with BSA more strongly than the ligands. Among the three

dx.doi.org/10.1021/ic2020308 | Inorg. Chem. 2011, 50, 12852−12866

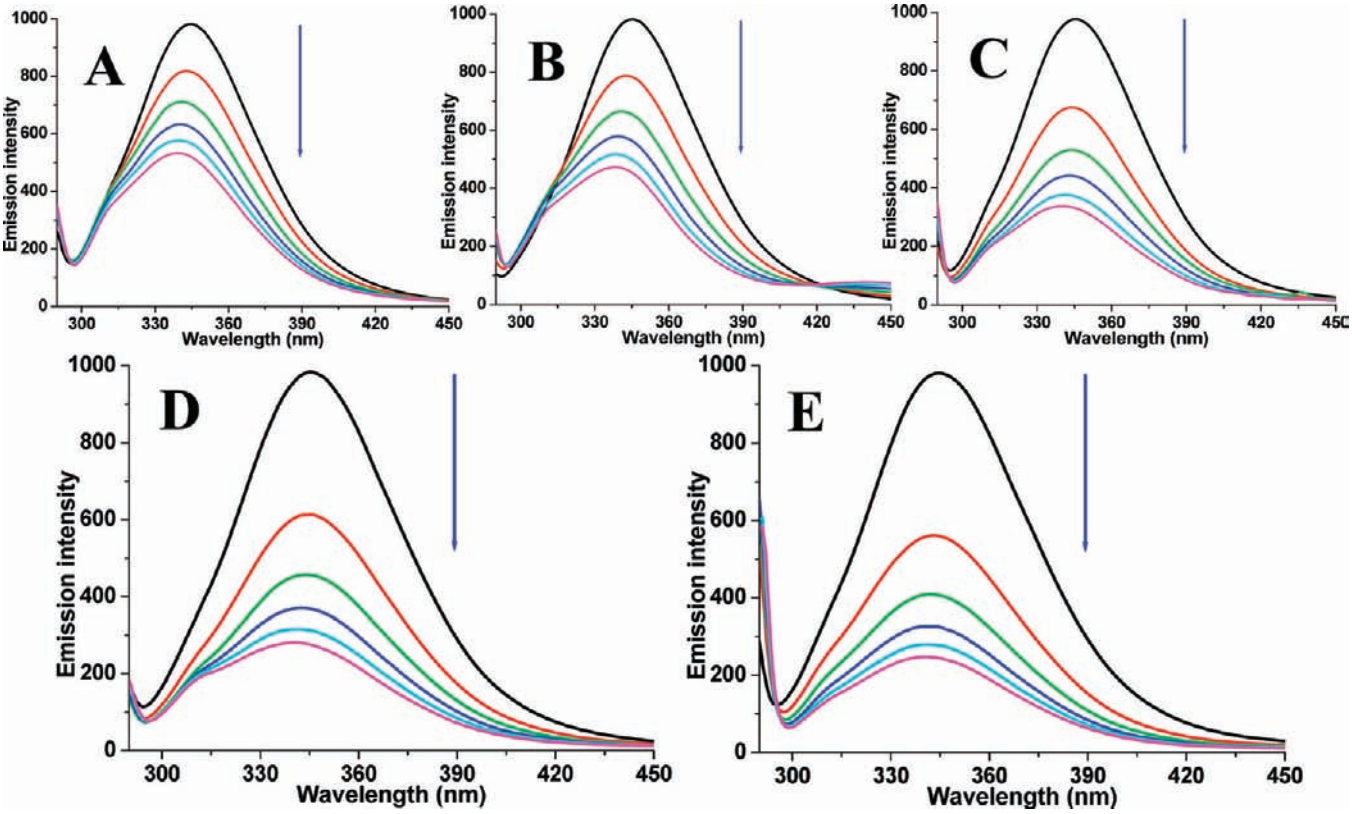

Figure 9. The emission spectrum of BSA (1 μM; λ_{exi} = 280 nm; λ_{emi} = 345 nm) in the presence of increasing amounts of compounds **1** (A), **2** (B), and **3** (C) (0, 10, 20, 30, 40, and 50 μM). The arrow shows the fluorescence quenching upon increasing the concentrations of the compounds.

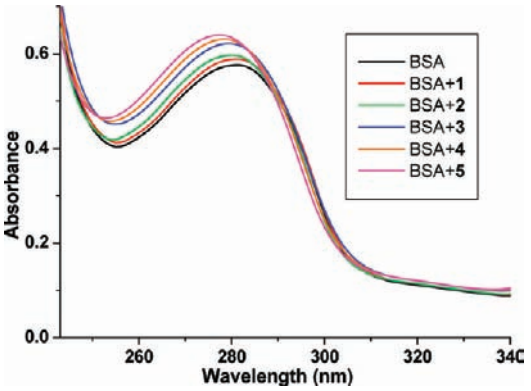

Figure 10. Absorption spectra of BSA (10 μM) and BSA with compounds **1**, **2**, **3**, **4**, and **5** (3 μM).

Table 2. Quenching Constant (K_q), Binding Constant (K_{bin}), and Number of Binding Sites (n) for the Interactions of Compounds with BSA

compound	K_q (M^{-1})	K_{bin} (M^{-1})	n
1	$1.68(\pm0.09) \times 10^4$	$4.85(\pm0.14) \times 10^4$	0.89
2	$2.16(\pm0.11) \times 10^4$	$7.76(\pm0.10) \times 10^4$	0.92
3	$8.81(\pm0.10) \times 10^4$	$4.18(\pm0.12) \times 10^5$	0.90
4	$2.01(\pm0.13) \times 10^5$	$8.31(\pm0.18) \times 10^5$	0.96
5	$5.90(\pm0.19) \times 10^5$	$2.63(\pm0.24) \times 10^6$	1.02

Cu(II) complexes, the cationic complex (**5**) has better interaction with BSA than the other two neutral complexes (**3** and **4**).

Characteristics of Synchronous Fluorescence Spectra. To investigate the structural changes that occurred for

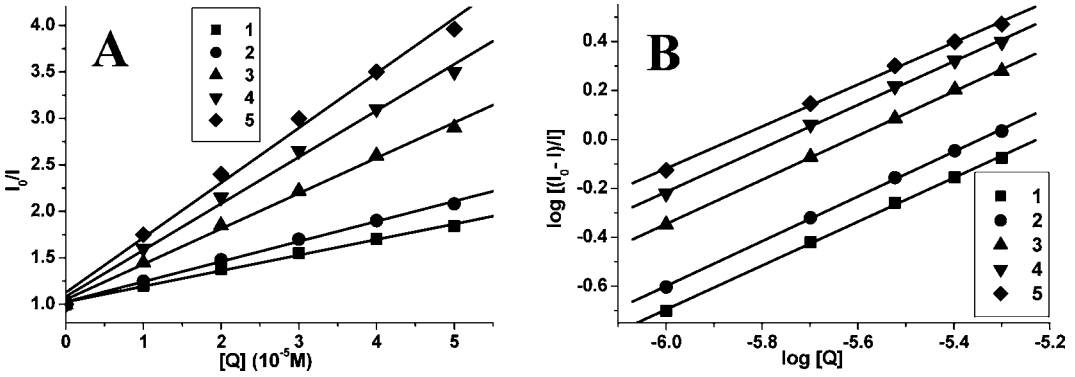

Figure 11. Stern–Volmer plots (A) and Scatchard plots (B) of the fluorescence titration of **1**, **2**, **3**, **4**, and **5** with BSA.

dx.doi.org/10.1021/ic2020308 | *Inorg. Chem.* 2011, 50, 12852–12866

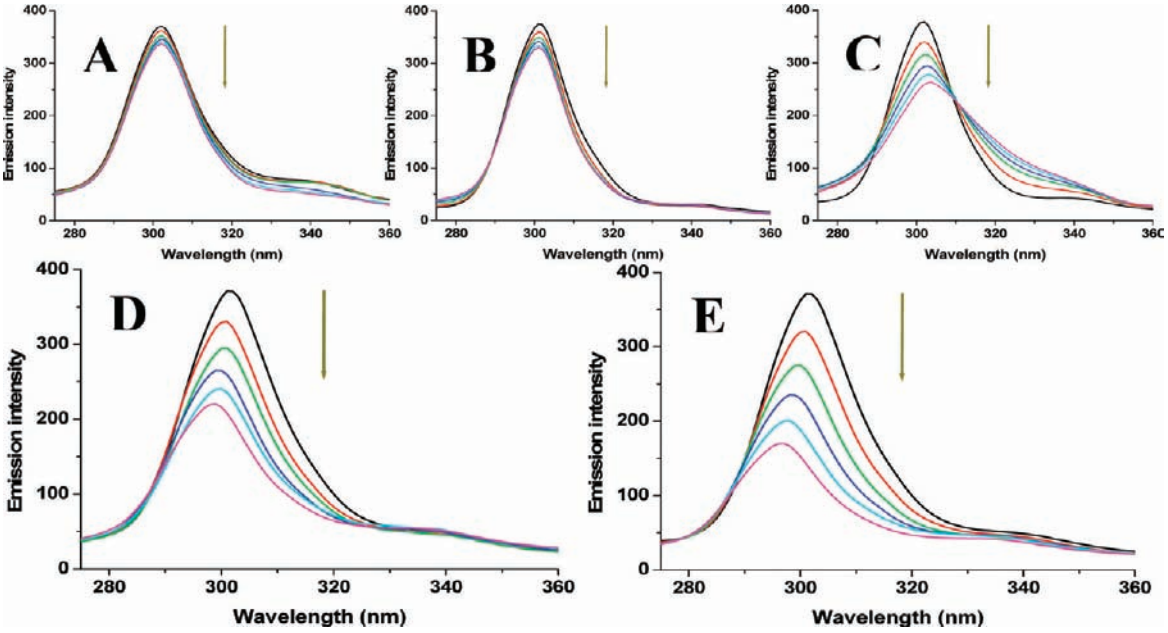

Figure 12. Synchronous spectra of BSA (1 μM) in the presence of increasing amounts of compounds **1** (A), **2** (B), **3** (C), **4** (D), and **5** (C) (0, 10, 20, 30, 40, and 50 μM) at a wavelength difference of $\Delta\lambda$ = 15 nm. The arrow shows the emission intensity changes upon the increase in concentration of the compounds.

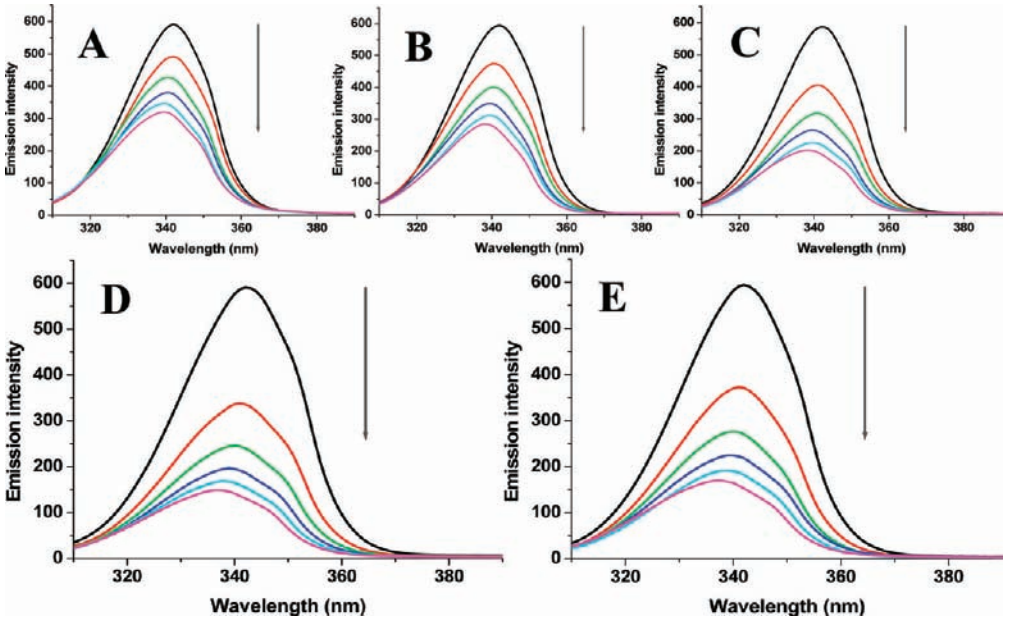

Figure 13. Synchronous spectra of BSA (1 μM) in the presence of increasing amounts of compounds **1** (A), **2** (B), **3** (C), **4** (D), and **5** (C) (0, 10, 20, 30, 40, and 50 μM) at a wavelength difference of $\Delta\lambda$ = 60 nm. The arrow shows the emission intensity changes upon the increase in concentration of the compounds.

BSA upon the addition of our compounds, synchronous fluorescence spectra of BSA were measured before and after the addition of test compounds to get valuable information on the molecular microenvironment, particularly in the vicinity of the fluorophore functional groups.[49] According to Miller,[50] in synchronous fluorescence spectroscopy, the difference between excitation and emission wavelength ($\Delta\lambda = \lambda_{emi} - \lambda_{exc}$) reflects the spectra of a different nature of chromophores. If the $\Delta\lambda$ value is 15 nm, the synchronous fluorescence of BSA is characteristic of tyrosine residue, whereas a larger $\Delta\lambda$ value of 60 nm is characteristic of tryptophan.[51]

The synchronous fluorescence spectra of BSA with various concentrations of test compounds were recorded at $\Delta\lambda$ = 15 nm and $\Delta\lambda$ = 60 nm and are shown in Figures 12 and 13, respectively. In the synchronous fluorescence spectra of BSA at $\Delta\lambda$ = 15, the addition of the compounds to the solution of BSA resulted in a small decrease of the fluorescence intensity of BSA at 302 nm, up to 9.1 and 11.6% of the initial fluorescence intensity of BSA for ligands **1** and **2**, respectively, with no shift in their emission wavelength maxima, but for complexes **3**, **4**, and **5**, the decrease in the intensity of the above mentioned band of about 30.6, 40.7, and 54.2% from the initial

dx.doi.org/10.1021/ic2020308 | *Inorg. Chem.* 2011, 50, 12852–12866

fluorescence intensity of BSA was accompanied by a blue shift of 2, 3, and 5 nm, respectively. At the same time, in the case of synchronous fluorescence spectra of BSA at $\Delta\lambda$ = 60, the addition of the compounds to the solution of BSA resulted in a significant decrease of the fluorescence intensity of BSA at 342 nm, up to 45.9, 52.1, 65.6, 75.2, and 78.7% of the initial fluorescence intensity of BSA accompanied with a blue shift of 3, 4, 3, 5, and 5 nm for compounds **1**, **2**, **3**, **4**, and **5**, respectively. The synchronous fluorescence spectral studies clearly suggested that the fluorescence intensity of tyrosine was not affected much with an increasing concentration of the ligands **1** and **2**, but the significant decrease along with a blue shift of fluorescence intensity of tryptophan has been observed. The results suggest that the interaction of ligands (**1** and **2**) with BSA affects the conformation of tryptophan only and not the tyrosine microregion. In the case of Cu(II) semicarbazone complexes **3**, **4**, and **5**, the fluorescence intensities of both the tryptophan and tyrosine were affected with an increasing concentration of the complexes, which clearly indicated that the interaction of complexes with BSA affects the conformation of both the tryptophan and tyrosine microregions.

Overall, the results of BSA protein binding experiments of our compounds revealed that the binding of compounds with BSA is mainly due to the hydrophobic and electrostatic interactions. The order of binding strength of the compounds with BSA is found to be **5** > **4** > **3** > **2** > **1**. This can explained by the fact that the hydrophobicity of **2** having phenyl substitution in its terminal nitrogen is greater than that of **1**; among the Cu(II) complexes, the complexes of N-phenyl substituted semicarbazone (**4** and **5**) have more hydrophobicity over that of complex **3**. In the case of binding strength of **4** and **5**, the electrostatic interaction has come into the picture; the cationic nature of **5** clearly has an edge over the neutral complex **4**. So, the strong interaction between the compounds and BSA suggested that these compounds can easily be stored in protein and will be released in desired targets; moreover, it could be interesting to study the pharmacological properties such as antioxidation and cytotoxicity of the compounds further.

Evaluation of Radical Scavenging Ability. Since the experiments conducted so far revealed that the ligands and its Cu(II) complexes exhibit good DNA and protein binding affinity, it is considered worthwhile to study the antioxidant activity of these compounds. The antioxidant properties of quinoline derivatives have attracted a lot of interest and have been extensively investigated, mainly in the *in vitro* systems.[52,53] The radical scavenging activities of our compounds along with standards such as butylated hydroxyanisole (BHA) and butylated hydroxytoluene (BHT) in a cell free system have been examined with reference to hydroxyl radicals ($OH^{\bullet}$), DPPH radicals ($DPPH^{\bullet}$), nitric oxide (NO), and superoxide anion radicals ($O_2^{-\bullet}$), and their corresponding IC_{50} values have been tabulated in Table 3. It is to be noted that no significant radical scavenging activities were observed in all of the experiments carried out with $CuCl_2$ and $Cu(NO_3)_2$, even up to 1.0 mmol of concentration under the same experimental conditions. The IC_{50} values (Table 3) indicated that the compounds showed antioxidant activity in the order of **5** > **4** > **3** > **2** > **1** in all of the experiments. In general, the $O_2^{-\bullet}$ scavenging power of the tested compounds was the greatest, and the NO scavenging was the least. The ligands (**1** and **2**) displayed almost comparable radical scavenging activity with respect to standard antioxidants (BHA and BHT) except in the case of $DPPH^{\bullet}$. But the three Cu(II) complexes exhibited nearly 5 to 100 times higher activity when compared to their corresponding ligands as well as the standards, which clearly indicated that the Cu(II) chelation plays a vital role in determining the antioxidative properties. Among the three Cu(II) complexes having the neutral ONO coordinated ligand, the more electron withdrawing nature and the planarity of the phenyl group should be the reason for the superior activity of **4** and **5** over **3**, whereas the highest activity for **5** might be due to the cationic nature of the square pyramidal complex (**5**) over the neutral octahedral complex (**4**).

Table 3. IC_{50} Values (in μM) Calculated from Various Radical Scavenging Assays of the Compounds (1, 2, 3, 4, and 5) and Standards (BHA and BHT)

compound	$OH^{\bullet}$	NO	$DPPH^{\bullet}$	$O_2^{-\bullet}$
1	321 ± 12	581 ± 5	161 ± 5	151 ± 8
2	273 ± 6	497 ± 9	123 ± 7	112 ± 3
3	49.8 ± 0.9	108 ± 3	48.9 ± 1.4	26.1 ± 1.5
4	19.2 ± 1.1	21.4 ± 0.7	10.3 ± 0.3	8.37 ± 0.14
5	8.23 ± 0.11	7.97 ± 0.16	5.21 ± 0.45	2.58 ± 0.97
BHA	315 ± 9	623 ± 10	9.89 ± 0.52	299 ± 7
BHT	277 ± 5	722 ± 9	9.17 ± 0.71	281 ± 9

***In Vitro* Cytotoxic Activity Evaluation of the Compounds.** The positive results obtained from the previous biological studies, namely, DNA binding and cleavage, BSA binding, and antioxidative studies for compounds **1**, **2**, **3**, **4**, and **5**, encouraged us to test their cytotoxicity against a panel of human cancer cell lines, human cervical cancer cells (HeLa), human laryngeal epithelial carcinoma cells (HEp-2), human skin cancer cells (A431), human liver carcinoma cells (Hep G2), and normal NIH 3T3 cells (mouse embryonic fibroblasts cells). Compounds were dissolved in DMSO, and blank samples containing same volume of DMSO were taken as controls to identify the activity of the solvent in this cytotoxicity experiment. Cisplatin was used as a positive control to assess the cytotoxicity of the test compounds. The results were analyzed by means of cell inhibition expressed as IC_{50} values and are shown in Table 4. It is to be noted that the ligands and the Cu(II) salts did not show any significant activity even up to a 500 μM concentration on all of the cells, which confirmed the chelation of the ligand with the Cu(II) ion being the only responsible factor for the observed cytotoxic properties of the new complexes. The IC_{50} values for **5** demonstrated a much higher inhibitory effect than that of **3** and **4**. The results of *in vitro* cytotoxic activity studies have also indicated that the IC_{50} value of three Cu(II) complexes against NIH 3T3 mouse embryonic fibroblasts (normal cells) is found to be above 250 μM, which confirmed that the complexes are very specific on cancer cells. In all of the cases, the activity of the three complexes has been found to be significantly lower than that of the well-known anticancer drug cisplatin. In general, Table 4 indicates that the three complexes have more cytotoxic specificity on human skin cancer cells over the other three cancer cells. Surprisingly, on comparison of the IC_{50} value of **5** with that of cisplatin against A431, the inhibitory activity of **5** against A431 is about three times higher than that of cisplatin. The Cu(II) complexes which possess superior cytotoxic properties over the ligands may be attributed to the extended planar structure induced by the $\pi \rightarrow \pi^*$ conjugation resulting from the chelating of the Cu(II) with the ligand. The overall cytotoxic behavior of the complexes is very similar to that of the

dx.doi.org/10.1021/ic2020308 | *Inorg. Chem.* 2011, 50, 12852–12866

Table 4. The Cytotoxic Activity of the Compounds

	IC_{50} values (μm)				
compound	HeLa	HEp-2	Hep G2	A431	NIH 3T3
3	47.7 ± 1.2	57.2 ± 2.4	37.1 ± 1.2	13.2 ± 1.7	265 ± 9
4	39.5 ± 1.7	34.3 ± 2.2	26.2 ± 0.7	12.4 ± 1.4	272 ± 6
5	13.2 ± 1.9	30.5 ± 3.3	19.3 ± 1.5	3.26 ± 0.12	255 ± 8
cisplatin	12.1 ± 0.6	14.7 ± 0.9	9.92 ± 0.43	10.3 ± 2.3	271 ± 9

DNA binding activity by them discussed earlier, indicating better activity for **5**.

CONCLUSION

The new ligand, 2-oxo-1,2-dihydroquinoline-3-carbaldehyde semicarbazone, its N(4)-phenyl derivative, and their three new copper(II) complexes have been prepared and well characterized by structural, analytical, and spectral methods. The presence of a phenyl group in the terminal nitrogen did not alter the coordination mode of semicarbazone, but the geometry of the copper(II) chloride complexes has been changed from square pyramidal to octahedral. The change of counterion (Cl^- to NO_3^-) in Cu(II) salts did not alter the coordination mode of the semicarbazone ligand (**2**), but there was a change in the geometry from octahedral to a square pyramidal one along with a change from the neutral to the cationic form of the resulting Cu(II) complexes. The DNA-binding properties of the free ligands and three Cu(II) complexes were investigated by absorption and fluorescence measurements. The results supported the fact that the compounds bind to CT-DNA via intercalation. The binding constants showed that the DNA binding affinity increased in the order **1** < **2** < **3** < **4** < **5**. The gel electrophoresis assay demonstrated that the complexes have been found to promote the cleavage ability of the pBR322 plasmid DNA by a hydrolytic cleavage mechanism. The protein binding properties of the compounds examined by the fluorescence spectra suggested that the binding affinity increases in the phenyl substitution at the terminal nitrogen of the semicarbazone moiety as well as the change of counterion (Cl^- to NO_3^-) in Cu(II) complexes, which could be explained on the basis of the hydrophobic and electrostatic interactions of the compounds with BSA. In addition, the complexes also exhibited excellent radical scavenging activities over the ligands, and the activity of **5** is better than that of **4** and **3**, which showed that the cationic nature of the complex increases the activity of the square pyramidal complex (**5**). Moreover, all three complexes showed considerable cytotoxic activity against HeLa, HEp-2, Hep G2, and A431 cancer cell lines without affecting the normal NIH 3T3 cells much. In particular, complex **5** showed excellent cytotoxic specificity against A431 cells. So, the overall structural and the pharmacological investigations strongly support the fact that the N(4) phenyl substitution in semicarbazone and the change of the counterion (Cl^- to NO_3^-) in Cu(II) salts have not only affected the structure and the nature of the complexes but also the various pharmacological properties of the resulting Cu(II) complexes. All encouraging chemical and biological findings indicate that complex **5** looks like a promising candidate as a live-cell imaging reagent that could contribute to the understanding of cellular uptake of metal complexes. Further studies are needed to assess their pharmacological properties *in vivo* and to elucidate the actual mechanism of the biological activity of **5**.

ASSOCIATED CONTENT

Supporting Information

Selected bond lengths (Å) and angles (deg) for **2**·CH_3OH, **3**, **4**, and **5** (Table S1); crystal packing diagram of the unit cell showing hydrogen bonding of **2**·CH_3OH, **3**, **4**, and **5** (Figures S1−S4); and changes in the electronic absorption spectra of **1** (A), **2** (B), and **4** (C) with increasing concentrations of CT-DNA (Figure S5). This material is available free of charge via the Internet at http://pubs.acs.org.

AUTHOR INFORMATION

Corresponding Author

*Tel.: +91 422 2428319. Fax: +91 422 2422387. E-mail: k_natraj6@yahoo.com.

ACKNOWLEDGMENTS

Financial assistance received from the Council of Scientific and Industrial Research, New Delhi, India [Grant No. 01(2216)/08/EMR-II and 21(0745)/09/EMR-II] is gratefully acknowledged. We would like to thank Dr. R. Sivasamy and Dr. J. Angayarkanni for their help in DNA cleavage experimental work (Department of Biotechnology, Bharathiar University, India). Acknowledgment is also made to Ms. N. Loganayaki and Prof. S. Manian, Department of Botany, Bharathiar University, India for their help in radical scavenging assays.

REFERENCES

(1) Boulikas, T.; Vougiouka, M. *Oncol. Rep.* **2003**, *10*, 1663−1682.
(2) Wong, E.; Giandomenico, C. M. *Chem. Rev.* **1999**, *99*, 2451−2466.
(3) Galanski, M.; Arion, V. B.; Jakupec, M. A.; Keppler, B. K. *Curr. Pharm. Des.* **2003**, *9*, 2078−2089.
(4) Wang, D.; Lippard, S. *J. Nat. Rev. Drug Discovery* **2005**, *4*, 307−320.
(5) Angeles-Boza, A. M.; Bradley, P. M.; Fu, P. K.-L.; Wicke, S. E.; Bacsa, J.; Dunbar, K. M.; Turro, C. *Inorg. Chem.* **2004**, *43*, 8510−8519.
(6) Foye, W. O. *Cancer Chemotherapeutic Agents*; American Chemical Society: Washington, DC, 1995.
(7) Bhat, S. S.; Kumbhar, A. A.; Heptullah, H.; Khan, A. A.; Gobre, V. V.; Gejji, S. P.; Puranik, V. G. *Inorg. Chem.* **2011**, *50*, 545−558.
(8) Rajendiran, V.; Karthik, K.; Palaniandavar, M.; Stockli-Evans, H.; Periasamy, V. S.; Akbarsha, M. A.; Srinag, B. S.; Krishnamurthy, H. *Inorg. Chem.* **2007**, *46*, 8208−8221.
(9) Primik, M. F.; Goschl, S.; Jakupec, M. A.; Roller, A.; Keppler, B. K.; Arion, V. B. *Inorg. Chem.* **2011**, *49*, 11084−11095.
(10) Krishnamoorthy, P.; Sathyadevi, P.; Cowley, A. H.; Butorac, R. R.; Dharmaraj, N. *Eur. J. Med. Chem.* **2011**, *46*, 3376−3387.
(11) Hegg, E. L.; Burstyn, J. N. *Coord. Chem. Rev.* **1998**, *173*, 133−165.
(12) Mancin, F.; Scrimin, P.; Tecilla, P.; Tonellato, U. *Chem. Commun.* **2005**, 2540−2548.
(13) Sigman, D. S.; Bruce, T. W.; Sutton, C. L. *Acc. Chem. Res.* **1993**, *26*, 98−104.
(14) Sigman, D. S. *Acc. Chem. Res.* **1986**, *19*, 180−186.
(15) Pogozelski, W. K.; Tullius, T. D. *Chem. Rev.* **1998**, *98*, 1089−1107.

(16) Armitage, B. *Chem. Rev.* **1998**, *98*, 1171−1200.
(17) Patra, A. K.; Dhar, S.; Nethaji, M.; Chakravarty, A. R. *Chem. Commun.* **2003**, 1562−1563.
(18) Dhar, S.; Senapati, D.; Das, P. K.; Chattopaddhyay, P.; Nethaji, M.; Chakravarty, A. R. *J. Am. Chem. Soc.* **2003**, *125*, 12118−12124.
(19) Dhar, S.; Chakravarty, A. R. *Inorg. Chem.* **2003**, *42*, 2483−2485.
(20) Thomas, A. M.; Nethaji, M.; Chakravarty, A. R. *J. Inorg. Biochem.* **2004**, *98*, 1087−1094.
(21) Reddy, P. A. N.; Santra, B. K.; Nethaji, M.; Chakravarty, A. R. *J. Inorg. Biochem.* **2004**, *98*, 377−386.
(22) Esposito, B. P.; Najjar, R. *Coord. Chem. Rev.* **2002**, *232*, 137−149.
(23) Khan, S. A. *Eur. J. Med. Chem.* **2008**, *43*, 2040−2044.
(24) Dutta, S.; Padhye, S.; Priyadarsini, K. I.; Newton, C. *Bioorg. Med. Chem. Lett.* **2005**, *15*, 2738−2744.
(25) Oliveira, R. B. d.; Souza-Fagundes, E. M. d.; Soares, R. P. P.; Andrade, A. A.; Krettli, A. U.; Zani, C. L. *Eur. J. Med. Chem.* **2008**, *43*, 1983−1988.
(26) Cerecetto, H.; Maio, R. D.; Gonzalez, M.; Risso, M.; Sagrera, G.; Seoane, G.; Denicola, A.; Peluffo, G.; Quijano, C.; Stoppani, A. O. M.; Paulino, M.; Olea-Azar, C.; Basombrio, M. A. *Eur. J. Med. Chem.* **2000**, *35*, 343−350.
(27) Dimmock, J. R.; Puthucode, R. N.; Smith, J. M.; Hetherington, M.; Quail, J. W.; Pugazhenthi, U.; Lechler, T.; Stables, J. P. *J. Med. Chem.* **1996**, *39*, 3984−3997.
(28) Dimmock, J. R.; Pandeya, S. N.; Quail, J. W.; Pugazhenthi, U.; Allen, T. M.; Kao, G. Y.; Balzarini, J.; Declercq, E. *Eur. J. Med. Chem.* **1995**, *30*, 303−314.
(29) Para, A.; Karolczyk-Kostuch, S. *Carbohydr. Polym.* **2002**, *48*, 55−60.
(30) Lee, W. Y.; Lee, P. P. F.; Yan, Y. K.; Lau, M. *Metallomics* **2010**, *2*, 694−705.
(31) Safavi, M.; Foroumadi, A.; Nakhjiri, M.; Abdollahi, M.; Shafiee, A.; Ilkhani, H.; Ganjali, M. R.; Hosseinimehr, S. J.; Emami, S. *Bioorg. Med. Chem. Lett.* **2010**, *20*, 3070−3073.
(32) Reddy, K. H.; Reddy, P. S.; Babu, P. R. *J. Inorg. Biochem.* **1999**, *77*, 169−176.
(33) Liu, Z.-C.; Wang, B.-D.; Yang, Z.-Y.; Li, Y.; Qin, D. D.; Li, T.-R. *Eur. J. Med. Chem.* **2009**, *44*, 4477−4484.
(34) Liu, Z.-C.; Wang, B.-D.; Li, B.; Wang, Q.; Yang, Z.-Y.; Li, T.-R.; Li, Y. *Eur. J. Med. Chem.* **2010**, *45*, 5353−5361.
(35) Raja, D. S.; Paramaguru, G.; Bhuvanesh, N. S. P.; Reibenspies, J. H.; Renganathan, R.; Natarajan, K. *Dalton Trans.* **2011**, *40*, 4548−4559.
(36) Raja, D. S.; Bhuvanesh, N. S. P.; Natarajan, K. *Eur. J. Med. Chem.* **2011**, *46*, 4584−4594.
(37) Singh, M. K.; Chandra, A.; Singh, B.; Singh, R. M. *Tetrahedron Lett.* **2007**, *48*, 5987−5990.
(38) Mabbs, F. E.; Machin, D. J. *Magnetism, Transition Metal Complexes*; Chapman and Hall: London, 1973.
(39) *APEX2*; BRUKER AXS Inc.: Madison, WI.
(40) Sheldrick, G. M. *SADABS*, version 2008/1; University of Göttingen: Göttingen, Germany, 2008.
(41) Blois, M. S. *Nature* **1958**, *29*, 1199−1200.
(42) Nash, T. *Biochem. J.* **1953**, *55*, 416−421.
(43) Green, L. C.; Wagner, D. A.; Glogowski, J.; Skipper, P. L.; Wishnok, J. S.; Tannenbaum, S. R. *Anal. Biochem.* **1982**, *126*, 131−138.
(44) Beauchamp, C.; Fridovich, I. *Anal. Biochem.* **1971**, *44*, 276−287.
(45) Blagosklonny, M.; EI-diery, W. S. *Int. J. Cancer* **1996**, *67*, 386−392.
(46) Zeng, Y. B.; Yang, N.; Liu, W. S.; Tang, N. *J. Inorg. Biochem.* **2003**, *97*, 258−264.
(47) Kobayashi, T.; Tobita, S.; Kobayashi, M.; Imajyo, T.; Chikira, M.; Yashiro, M.; Fujii, Y. *J. Inorg. Biochem.* **2007**, *101*, 348−361.
(48) Hu, Y.; Yang, Y.; Dai, C.; Liu, Y.; Xiao, X. *Biomacromolecules* **2010**, *11*, 106−112.
(49) Chen, G. Z.; Huang, X. Z.; Zheng, Z. Z.; Xu, J. G.; Wang, Z. B. *Methods of Fluorescence Analysis*, 2nd ed.; Science Press: Beijing, 1990.
(50) Miller, J. N. *Proc. Anal. Div. Chem. Soc.* **1979**, *16*, 203−208.
(51) Tang, J. H.; Luan, F.; Chen, X. G. *Bioorg. Med. Chem.* **2006**, *49*, 3210−3217.
(52) Sankaran, M.; Kumarasamy, C.; Chokkalingam, U.; Mohan, P. S. *Bioorg. Med. Chem. Lett.* **2010**, *20*, 7147−7151.
(53) Malakyan, M. G.; Badzhinyan, S. A.; Vardevanyan, L. A.; Grigoryan, D. S.; Egiazaryan, D. E.; Avetisyan, A. A; Aleksanyan, I. L; Ambartsumyan, L. P.; Sargsyan, K. S. *Pharm. Chem. J.* **2009**, *43*, 8−11.